Project title: Implications of Medical Low Dose Radiation Exposure

Grant Agreement Number: 755523

Call identifier: NFRP-2016-2017

Topic: NFRP-9

Deliverable D2.23

Accelerated Monte Carlo code for an online patient monitoring system in interventional cardiology procedures

Lead partner: Universitat Politècnica de Catalunya (UPC)

Author(s): D. Fernández-Bosman, M. Ginjaume, M.A. Duch (UPC)

J. Dabin, F. Vanhavere (SCK CEN)

Work Package: 2

Estimated delivery: 30 May 2021

Actual delivery: 2 June 2021

Type: Report

Dissemination level: Public

This project has received funding from the Euratom research and training programme 2014-2018 under grant agreement No 755523.

Table of contents

List of figures

List of tables

1. Introduction

Nowadays interventional radiology and cardiology are among the medical specialties that are most commonly used because of their minimally invasive procedures. However, the X-rays employed during fluoroscopically guided procedures in order to generate medical images entail high exposure to the patient and the possibility of suffering deterministic effects. In this regard, the 2013/59/EURATOM Directive establishes basic safety standards for protection against dangers arising from exposure to ionizing radiation [1]. In article 60, it is specified that any equipment used for interventional radiology must have a device or a feature informing the practitioner, at the end of the procedure, of relevant parameters for assessing patient dose.

The objective of MEDIRAD Subtask 2.2.2 is to develop a real time patient dose monitoring application for interventional cardiology procedures based on the freely available accelerated Monte Carlo (MC) code, MC-GPU [2]. In particular, to validate and improve MC-GPU to determine patient skin dose distribution and organ doses for specific realistic clinical set-up in interventional radiology.

When MEDIRAD started, MC-GPU had not yet been validated against measurements. The main actions performed in the framework of MEDIRAD subtask 2.2.2 have been:

1.- Optimization and up-date of MC-GPU latest publicly available version, released in 2012 (MC-GPU v1.3, available at *https://code.google.com/archive/p/mcgpu/.*

2.- Development of PyMCGPU-IR which integrates MC-GPU improvements and an application to prepare MC-GPU source input files from the X-ray console [3] (MEDIRAD MS41)

3.- Comparison of MC-GPU dose calculations with a well-validated MC simulation code and with measurements carried out with simple phantoms in a calibration laboratory and under realistic conditions in an operating room [4].

4.- Comparison of MC-GPU dose calculations with measurements in realistic interventional radiology procedures.

This deliverable summarizes the improvements introduced in MC-GPU code and describes PyMCGPU-IR as a new tool for patient dose calculation for interventional procedures. It also summarizes the main results of the validation studies and describes a demo that has been prepared to test the developed application.

2. MC-GPU

MC-GPU is a Monte Carlo simulation code that can generate synthetic radiographic images of realistic models of the human anatomy using the computational power of commodity Graphics Processing Unit cards. The code implements a massively multithreaded Monte Carlo simulation algorithm for the transport of X-rays in a voxelized geometry. The X-ray interaction models and material properties have been adapted from PENELOPE 2006 [5]. The code was first developed by Badal et al 2009 [2], using the CUDA 2.2 programming model and PENELOPE 2006 photon interaction model. This version was available in the public domain since 2010. In 2012, MC-GPU, v.1.3, was upgraded to CUDA 5, but no changes on the physics were introduced.

2.1 Improvements in physics model

The PENELOPE simulation algorithm has been successively updated since MC-GPU first publication. In the framework of MEDIRAD, relevant data on materials for MC-GPU have been updated to physics models from PENELOPE, 2014 [6]. For the energy range taken into consideration (20 to 120 keV), the main change between the 2014 and 2006 versions mainly consisted of new cross sections implemented for Rayleigh and photoelectric effects. Differences in the total mean free paths are small at low energies (2-3% depending on the material of interest) and almost negligible for high energies. However, updating the materials description is relevant for this study since photoelectric interactions are predominant at the typical energy range of interventional cardiology.

2.2 Other improvements

In addition, a set of functions were developed to automatically set the optimal values for the GPU calculations (number of blocks per kernel, number of threads per block, number of histories per thread to be simulated by the GPU). The new version of MC-GPU with the above improvements and focussed for its application in interventional radiology is renamed, in agreement with A. Badal, as MCGPU-IR.

3. PyMCGPU-IR

3.1 Introduction to PyMCGPU-IR

MCGPU-IR uses an independent computer code as the virtual X-ray control console where the user manually introduces the relevant acquisition parameters, such as tube voltage (kVp), filtration, collimation, gantry position and angulation. This is a limitation for its use in the clinics since a typical interventional procedure requires tens or even hundreds of events and it is not practical to introduce them manually.

The automatic acquisition of X-ray source conditions from console module in interventional cardiology has been achieved through the development of PyMCGPU-IR. PyMCGPU-IR is a Python[1] application for MCGPU-IR for patient dose calculation in interventional radiology. It reads several input data files (e.g. Radiation Dose Structured Reports, RDSR [7]) to retrieve the required information about each irradiation event and to transform them into MCGPU-IR input files, then proceeds to launching the simulation, and finally retrieves the radiation doses from its output. As MCGPU-IR does not parse RDSR files, before PyMCGPU-IR all these processes had to be done manually. MEDIRAD Milestone 41 provides details about the automatic acquisition system [3]. We here present the PyMCGPU-IR version of 2021. A paper to be submitted in Physica Medica is in progress.

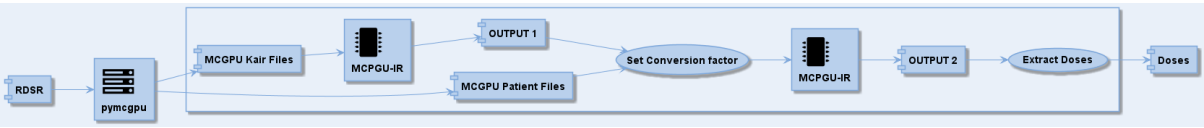

Figure 1: PyMCGPU-IR flow chart

3.2 PyMCGP-IR Requirements

PyMCGPU-IR can be distributed as a binary application; in order to use it the requirements of MCGPU-IR need to be fulfilled, plus a copy of MCGPU-IR. To use it from source code the main requirement is to have Python 3.6 or newer, a computer/cluster with NVIDIA GPUs capable of running with CUDA 8 and the MPI and LCM libraries.

3.3 Features of PyMCGP-IR

Clustering of events

In a typical interventional radiology procedure, once the C-arm is positioned to irradiate the region of interest in the patient's body and the X-ray beam has been tuned to obtain a clear image, the operator may remain in the same configuration for a while doing single irradiations events with only slight modifications until he needs to irradiate from another direction or a new region of interest. This means that there may be sets of events with only slight differences in the radiological parameter values. MCGPU-IR calculates the doses for each single event separately. To reduce calculation time, a clustering algorithm has been developed to group these sets of events into single ones, as the slight differences among the events lead to negligible differences in the simulations, thus reducing the

[1] Python is an interpreted high-level general-purpose programming language. See https://www.python.org/

number of total events to be simulated by MCGPU-IR. This algorithm has been implemented into PyMCGPU-IR.

Supported RDSR file formats

Radiation Dose Structured Report (RDSR or SR) stores information of each irradiation event made during a procedure including also patient information, study information and manufacturer proprietary information.

RDSR is generated by the X-Ray machine and stored internally or in a hospital picture archiving and communication system (PACS). Although the report is generated in a standard format, it may not be retrieved in the same format.

PyMCGPU-IR supports reading RDSR in different formats: the standard DICOM format (.dcm, .sr), and spreadsheet format, namely, Microsoft Excel file format (.xls) and Office Open XML file formats (.xlsx).

Information retrieval from RDSR

Prior to calculation, RDSR files have to be read in order to retrieve the information relevant for the dose calculation. Figure 2 shows the information, which is extracted from the RDSR. Once retrieved, information needs to be converted to the representation or file format expected by the dose calculation program, MCGPU-IR.

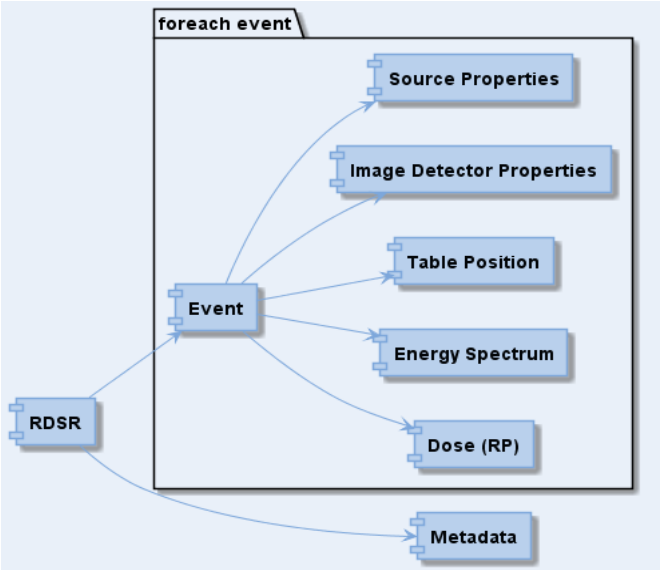

Figure 2: Information retrieved from the RDSR file

RDSR supplement

Despite the RDSR being a standard, there are some fields, especially those related to the relative position of the patient with respect to the beam source, that are treated differently depending on the specific machine. In addition, in some cases the RDSR does not provide all the required information, either because it was anonymized, and patient gender is missing, or it was incomplete because the clinician did not introduce some data such as patient height or weight. Moreover, for accuracy of the dose calculation, information about the exact radiation source model is required. In order to bypass these issues, PyMCGPU-IR supports reading another file which is created by the person in charge of the dose calculation and it is used to supplement the RDSR. This file may contain information about the patient, X-Ray source parameters and the relative position between patient and the X-Ray source.

Patient phantom

PyMCGPU-IR models the patient using the REX and REGINA anthropomorphic phantoms, developed by Helmholtz Zentrum München, [8, 9] for male and female patients, respectively. Although ICRP did not adopt these names, REX and REGINA correspond to the ICRP Adult voxel phantoms [10], male and female respectively. In PyMCGPU-IR, both phantoms are segmented in 27 different materials corresponding to different organs and tissue materials.

Both phantoms can be rescaled to better fit the patient height and weight.

3.3 Reporting patient dose

The main objective of the simulation is the calculation of patient doses, these have to be reported by organs or even with higher granularity in order to visualize them graphically.

The granularity is defined by the accuracy of the voxelized geometry used to represent the patient. The voxel size will define the accuracy of the volume of the organs and the tags the ability to identify them. PyMCGPU-IR outputs accumulated doses per tag and event and their total and stores as file the deposited voxel doses per irradiation event.

Figure 3 shows a screen capture of the output results of PyMCGPU-IR. Column one of Figure 3 corresponds to the tag which identifies the material. The correspondence between the Tags and the materials is given in the list below Figure 3. Tag 7 is associated to the back skin. In columns 2, 3 and 4, the mean doses per organ (in µGy) together with the associated statistical uncertainty for "*k=2*" in absolute value and percentage are given. Columns 5, 6 and 7 report the peak organ dose for each organ together with the associated uncertainties. Column 8 is the peak organ dose location. Column 9 is the total energy deposited in the organ in units of µGy·g. Finally, columns 10 and 11 are the total organ mass and the total number of voxels for the given organ, respectively.

>>>>>>>>>> FINAL REPORT: TOTAL *PATIENT* VOXEL DOSE >>>>>>>>>>

*** VOXEL ROI DOSE TALLY REPORT ***

Dose deposited in the different materials inside the input ROI computed post-processing the 3D voxel dose results.

[MAT]	[Mean Organ Dose µGy]	[2*std_dev]	[U(%) (k=2)]	[Peak Organ Dose µGy]	[2*std_dev]	[U(%) (k=2)]	[Peak voxel coord]	[E_dep µGy·g]	[MASS_ROI g]	[NUM_VOXELS_ROI]
1	7.589159e+02	4.483349e-01	0.059	4.834667e+05	1.392037e+04	2.879	(148,11,172)	1.742427e+05	2.295943e+02	5215248
2	3.373168e+04	1.655214e-02	0.000	1.487040e+06	0.000000e+00	0.000	(129,23,168)	1.500865e+08	4.449423e+03	63216
3	7.864569e+03	2.064087e-02	0.000	4.742698e+05	0.000000e+00	0.000	(129,25,172)	4.557363e+07	5.794803e+03	137314
4	2.924237e+04	0.000000e+00	0.000	9.878829e+04	0.000000e+00	0.000	(103,56,167)	2.441964e+07	8.350775e+02	21769
5	5.482180e+03	1.206761e-02	0.000	4.112472e+05	0.000000e+00	0.000	(139,16,171)	1.347621e+08	2.458185e+04	646967
6	1.150707e+03	7.880541e-02	0.007	1.277992e+04	0.000000e+00	0.000	(55,88,164)	8.004487e+05	6.956147e+02	17468
7	2.238454e+04	7.559446e-02	0.000	4.089476e+05	0.000000e+00	0.000	(144,15,172)	1.722279e+07	7.694052e+02	19321
8	5.864430e+02	3.166681e-02	0.005	1.718279e+05	0.000000e+00	0.000	(55,33,164)	1.417439e+06	2.417010e+03	60695
9	4.275220e+04	3.157688e-02	0.000	2.253736e+05	0.000000e+00	0.000	(98,32,165)	3.952050e+07	9.244086e+02	45615
10	5.328892e+03	9.535715e-03	0.000	3.867481e+05	0.000000e+00	0.000	(144,18,171)	1.545181e+08	2.899628e+04	755882
11	2.557259e+03	1.639466e-01	0.006	2.010204e+05	0.000000e+00	0.000	(109,30,167)	3.714109e+05	1.452379e+02	3614
12	1.067731e+04	4.909376e-02	0.000	8.963250e+04	0.000000e+00	0.000	(141,38,170)	6.907636e+06	6.469456e+02	43108
13	2.254724e+04	1.968637e-01	0.001	5.964175e+04	0.000000e+00	0.000	(119,55,169)	9.106656e+05	4.038923e+01	1063
14	2.244442e+03	3.063481e-01	0.014	3.929426e+03	0.000000e+00	0.000	(115,73,184)	4.485661e+04	1.998564e+01	526
15	1.199526e+01	6.309224e-02	0.526	4.758109e+01	1.005600e+01	21.134	(138,109,207)	3.086373e+03	2.572994e+02	6770
16	3.887581e+03	3.988759e-02	0.001	2.566619e+04	0.000000e+00	0.000	(125,71,160)	6.996776e+06	1.799776e+03	46917
17	4.335983e+02	1.030808e-01	0.024	5.296514e+03	2.104305e+01	0.397	(39,52,168)	1.207948e+05	2.785868e+02	7781
18	2.871698e+03	6.563920e-01	0.023	6.625219e+03	0.000000e+00	0.000	(67,107,166)	4.305713e+04	1.499362e+01	432
19	3.270742e+03	8.607979e-01	0.026	7.449801e+03	0.000000e+00	0.000	(66,109,166)	3.266483e+04	9.986976e+00	268
20	9.474189e+02	1.067793e-01	0.011	1.263940e+04	0.000000e+00	0.000	(79,71,157)	5.683673e+05	5.999112e+02	15789
21	1.327930e+04	6.588468e-02	0.000	7.754730e+04	0.000000e+00	0.000	(101,56,161)	5.310936e+06	3.999408e+02	10526
22	6.724721e-01	3.966994e-02	5.899	6.460939e+00	5.145764e+00	79.644	(122,85,102)	2.353240e+01	3.499387e+01	921
23	2.343116e+02	3.168051e-01	0.135	6.219949e+02	1.375674e+01	2.212	(108,82,193)	1.990920e+04	8.496894e+01	2258
24	6.544004e+01	5.978723e-02	0.091	4.077835e+02	1.317596e+01	3.231	(118,38,207)	9.487564e+04	1.449810e+03	37794
25	3.860586e+01	3.939916e+00	10.206	5.066903e+01	1.055802e+01	20.837	(109,115,208)	7.404617e+00	1.918043e-01	5
26	2.058741e+01	2.776635e+00	13.487	2.548793e+01	7.094755e+00	27.836	(138,116,208)	3.948753e+00	1.918043e-01	5
27	3.836226e+03	0.000000e+00	0.000	3.960404e+03	0.000000e+00	0.000	(126,114,164)	5.830376e+02	1.519821e-01	4
28	4.599523e+04	0.000000e+00	0.000	3.143503e+06	0.000000e+00	0.000	(152,9,173)	5.114643e+08	1.111994e+04	112776
29	1.244006e+04	3.616867e+00	0.029	8.507224e+05	1.871513e+04	2.200	(150,2,173)	2.779314e+05	2.234165e+01	507492

Figure 3: Example of PyMCGPU-IR output for a given event

List of Tags and materials in PyMCGPU-IR:

- Tag1: Outer Air.
- Tag2: Cortical Bone.
- Tag3: Spongious Bone.
- Tag4: Heart.
- Tag5: Remaining Tissue.
- Tag6: Front Skin.
- Tag7: Back Skin.
- Tag8: Other Skin.
- Tag9: Blood.
- Tag10: Muscle.
- Tag11: Cartilage.
- Tag12: Lung.
- Tag13: Oesophagus.
- Tag14: Thyroid.
- Tag15: Bladder.
- Tag16: Liver.
- Tag17: Medula.
- Tag18: Breast Adipose.
- Tag19: Breast Glandular.
- Tag20: Colon.
- Tag21: Stomach.
- Tag22: Gonads.
- Tag23: Salivary Glands.
- Tag24: Brain.
- Tag25: Eye Lens Left.
- Tag26: Eye Lens Right.
- Tag27: Hp(10).
- Tag28: Aluminium Table.
- Tag29: Air below Table.

The output is a stream of data, and the accumulated dose is represented in tabular format when it is ready. In order to retrieve it, PyMCGPU-IR parses the output and extracts the values for each tag and event.

PyMCGPU-IR stores aggregated doses into a single file, identifying each event by its date and time. This file can be stored as spreadsheet (Excel) or javascript object notation (JSON)[2].

[2] JSON is text based syntax for data interchange, defined with the standards ECMA-404, ISO/IEC 21778:2017 and STD-90.

4. PyMCGPU-IR validation

PyMCGPU-IR validation included two parts. First the improvements of MC-GPU were verified by comparing MCGPU-IR[3] results with a "multipurpose MC code" and with simple irradiation events. The results are presented in paragraphs 4.1 and 4.2. In these examples, the phantoms and the radiation sources are introduced manually, the purpose is to verify the radiation transport algorithm in simple situations. The second validation described in paragraph 4.3 corresponds to the verification of the complete PyMCGPU-IR application, including the automatic acquisition of the X-ray source data and the clustering of events.

All uncertainties indicated in this paragraph have been calculated following the recommendations of the Guide to the Expression of Uncertainty in Measurement (GUM) [11]. All sources of uncertainty associated to a given measurement are evaluated and combined to obtain the range of dispersion of the measurand. In order to have a confidence level of approximately 95%, an expanded uncertainty is calculated, multiplying the standard uncertainty by a coverage factor, *k,* equal to 2.

4.1 Comparison with "general purpose" MC code

The code used for MCGPU-IR validation was PENELOPE/penEasy (version 2014 and version 2015, respectively). PENELOPE [6] is one of the available reference codes for the Monte Carlo simulation of electron, positron and photon transport. penEasy [12] is a general-purpose main program defined specifically for PENELOPE. It provides the user with a set of source models and tallies which are invoked from a structured code. In this comparison, organ doses and doses at voxel level are calculated with both programs.

The thorax of an anthropomorphic phantom from the Virtual family [13] is completely irradiated using a known X-ray source. The Duke phantom which represents a 34-year-old-male and has 122x62x372 voxels of dimensions 0.5x0.5x0.5 cm^3 is used in the comparison. More details can be found in Fernández-Bosman et al. [4].

The PENELOPE/penEasy code needed 33529 seconds of execution time in order to complete the simulation and achieve standard errors of about 0.1% (*k*=2). On the other hand, MC-GPU took approximately 13 seconds (execution time). Furthermore, both programs identify the maximum voxel dose at the same position, that is, in the air at the entrance of the patient. The difference between the Peak Skin Dose (PSD) reported by both codes was only 0.6% with an associated statistical uncertainty (*k*=2) of 1% for MC-GPU and 2 % for PENELOPE/penEasy. Both codes reported the same location of the PSD.

4.2 Comparison with measurements in simple set-ups

Two experiments were undertaken. First of all, a series of irradiations with IEC 61267 RQR reference radiation qualities [14] were performed at the UPC Calibration Laboratory under controlled conditions. Subsequently a second set of irradiations were performed in a realistic environment at the Hemodynamic Department of the Hospital Universitari Vall d'Hebron (HUVH), simulating a clinical scenario. The experimental measurements were performed with thermoluminescent (TL) dosimeters.

[3] MCGPU-IR is the new version of MC-GPU which includes the improvements described in paragraph 2 (see paragraph 2.2.). It is distributed together with PyMCGPU-IR

Slab phantoms made of different tissue-equivalent materials were used. Some of these plates have small cavities where the TL detectors can be accommodated. The materials of the plates were plastic water (PW®, ρ=1.03 g/cm^3), lung tissue-equivalent material (ρ=0.199 g/cm^3) and bone tissue-equivalent material (ρ=1.93 g/cm^3) from Computerized Imaging Reference Systems (CIRS). Lung and bone equivalent materials match the linear attenuation coefficients of their reference tissues [15] to within +/- 2.5%. Nine detectors were irradiated at each measurement position and the measured dose to be compared to the simulation is then obtained as the average of the nine readings. The materials were simulated according to the atomic composition specified by the manufacturer and the slab phantoms were modelled in MCGPU-IR for the purpose of the validation

Differences between the simulated and the UPC lab experimental dose values were below 5%, except for the lung and one of the tested qualities (RQR6, [14]), where a difference of 6% was obtained. Simulation time ranged between 50 and 100 s, depending on the setup.

Good agreement was also observed between the simulated and the hospital experimental doses. Differences were below 15% and within the associated uncertainty (13%-18%). In this second set of experiments, the uncertainty was higher both for the measurements and for the calculations. On the one hand, the X-ray beam and the energy response of the TLDs is less well known than in a calibration lab. On the other hand, the calculations have to be normalized to the KAP recorded in the RDSR.

4.3 Comparison with realistic set-ups

The last step for the complete validation was to use PyMCGPU-IR and simulate complex realistic procedures with different projections. The experiments were performed at the Centre hospitalier universitaire de Liège in Belgium. Measurements were performed with TLDs in a Rando Alderson anthropomorphic phantom. A first set of three measurements consisted of placing several TLD arrays on the back of the Rando Alderson to measure the PSD and the skin dose distribution. Three sets of projections were investigated (Table 1). The first irradiation was performed in posterior anterior (PA) configuration only. The two other irradiation events were a combination of up to three projections (PA, left lateral oblique (LAO) and cranial (CRAN)).

For PA projection, 3 TLDs forming a triangle were placed on the back skin of the phantom. For the other two experimental setups, a squared array of 5*5 detectors were used.

The second set of measurements consisted of three complete cardiac procedures, with 108, 25 and 25 events, respectively. TLDs were placed in 4 different slices (slice 15 to 18) at the right and left lung and the oesophagus level to measure the absorbed dose. Figure 4 is an example of the position of the TLDs for slice 15. The same position of the TLDs was used for the three procedures. There was 1 TLD at the oesophagus, 2 TLDs at the right lung and 2 or 3 detectors at the left lung, depending on the slice.

For the comparison of PyMCGPU-IR with TLD measurements, the Alderson-Rando phantom with its different slices and holes was used in the simulation. The skin dose data were obtained irrespectively with the Alderson-Rando and the REX phantom. In this deliverable, the results corresponding to the peak skin dose calculations were obtained using the REX phantom. No differences were observed when using the Alderson-Rando phantom.

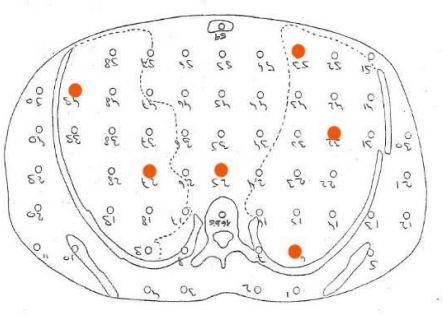

Figure 4: Example of distribution of TLDs in slice 15

Results for peak skin dose calculation

Table 1 shows the measured and calculated maximum skin dose for the first set of measurements. For the PA projection, since there were only 3 TLDs and they were all homogeneously irradiated the mean value has been included in the results. As an example, Figure 5 shows the peak skin dose and the skin dose distribution for the last irradiation event which is a combination of three projections: PA + LAO 20 + PA CRAN 15º.

The differences between calculations and TL measurements for the peak skin dose varied within ±6%, and were consistent with the associated uncertainty.

Table 1: Comparison of measurements and dose calculations for the first set of measurements

Projections*	**TLD measurements**		**PyMCGPU-IR calculation**		**Ratio:** $\frac{\textbf{PyMCGPU}-\textbf{IR}}{\textbf{TLDs}}$	**Execution time**
	PSD (mGy)	**U(%) (*k*=2)**	**PSD (mGy)**	**U (%) (*k*=2)**		(s)
PA**	337	20%	354	21%	1.05	90
PA + LAO 20º	512	20%	481	15%	0.94	180
PA+LAO 20º + PA CRAN 15 º	727	20%	742	12%	1.02	270

* PA: Postero-anterior; LAO: Left lateral oblique; CRAN: Cranial

** In this case, the tabulated values correspond to the mean dose

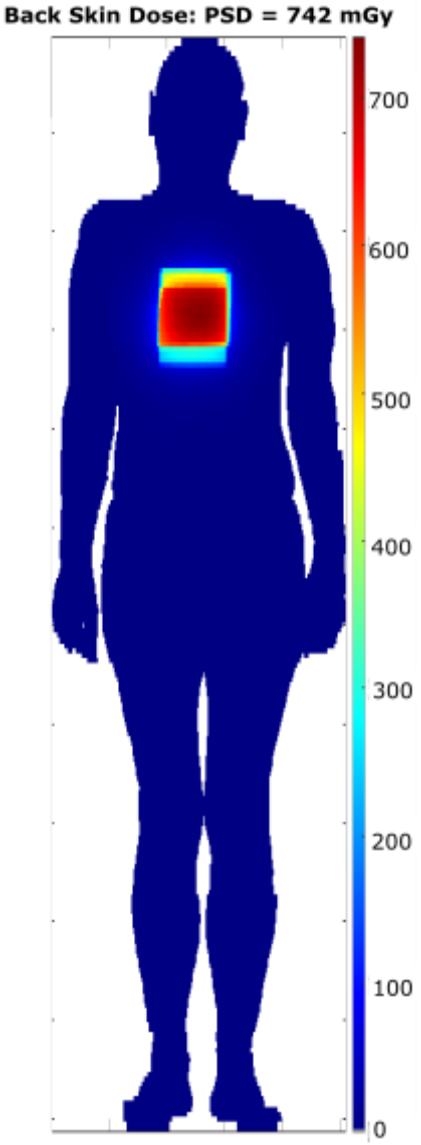

Figure 5: Skin dose distribution for the (PA + LAO 20 + PA CRAN 15º) projection. Voxel size of 0.2137 x 0.2137 x 0.8 cm^3

Results: organ dose calculation4

Results from the three clinical procedures are presented below. Set 1 corresponded to 108 events that were reduced to 11, after applying the clustering algorithm. The calculation time was 15 minutes. Set 2 corresponded to 25 events reduced to 8 calculations. The calculation time was 12 minutes. Set 3 corresponded to 25 events which were reduced to 7 calculations. The calculation time was 10.5 minutes.

[4] In this paragraph we consider the "organ dose", as the mean dose derived from the TLDs measurements, but the number of TLDs is too small and the radiation field too inhomogeneous to really measure the organ dose. In the calculations, for the purpose of the validation, the same criteria are followed, but the program can calculate the organ dose and the dose distribution in the organ, provided that the organ is segmented in the phantom.

Tables 2, 3 and 4 summarize the main results. In these simulations, the Alderson-Rando phantom was modelled to identify the measurement point. For each procedure, we present the measured and calculated absorbed dose in each slice and organ, the associated uncertainties and the ratio between calculation and measurement. We also present the average of the organ dose calculated as the mean value of the different slices. The average indicated in the column "ratio" of the Tables is calculated as the ratio of the average of the calculated dose and the average of the measured dose in each organ.

Table 2: Comparison of the measured mean dose of the left lung, right lung and the oesophagus with the corresponding calculated doses for SET 1

SET 1		**TLD measurement**		**PyMCGPU-IR**		**Calculation/measurement**	
Organ	**Slice**	**dose (mGy)**	**U(%) (*k=2*)**	**dose (mGy)**	**U(%) (*k=2*)**	**Ratio**	**U(%) (*k=2*)**
Left Lung	15	15.0	15%	12.7	15%	0.85	22%
	16	75.6	17%	90.4	8%	1.20	19%
	17	115.1	14%	107.7	6%	0.94	15%
	18	94.0	17%	90.5	7%	0.96	18%
	Average	**74.9**	**9%**	**75.3**	**4%**	**1.01**	**10%**
Right Lung	15	22.3	16%	47.6	9%	2.13	18%
	16	26.5	19%	20.3	14%	0.76	23%
	17	18.1	20%	16.7	24%	0.92	31%
	18	28.0	19%	27.5	13%	0.98	23%
	Average	**23.7**	**9%**	**28.0**	**7%**	**1.18**	**11%**
Oesophagus	15	22.6	20%	34.5	12%	1.53	23%
	16	50.9	20%	58.3	13%	1.14	24%
	17	57.6	20%	71.8	12%	1.25	23%
	18	70.0	20%	74.1	12%	1.06	23%
	Average	**50.3**	**11%**	**59.7**	**6%**	**1.19**	**12%**

Table 3: Comparison of the measured mean dose of the left lung, right lung and the oesophagus with the corresponding calculated doses for SET 2

SET 2		TLD measurement		PyMCGPU-IR		Calculation/measurement	
Organ	**Slice**	**dose (mGy)**	**U(%) (*k=2*)**	**dose (mGy)**	**U(%) (*k=2*)**	**Ratio**	**U(%) (*k=2*)**
Left Lung	15	9.7	14%	10.7	14%	1.10	20%
	16	95.1	15%	95.0	7%	1.00	17%
	17	136.7	14%	123.6	5%	0.90	15%
	18	117.8	16%	95.4	7%	0.81	17%
	Average	**89.8**	**9%**	**81.2**	**4%**	**0.90**	**9%**
Right Lung	15	43.6	15%	51.3	9%	1.18	17%
	16	18.1	18%	17.8	14%	0.99	23%
	17	15.8	20%	14.3	24%	0.90	31%
	18	22.3	18%	37.0	11%	1.66	22%
	Average	**24.9**	**9%**	**30.1**	**6%**	**1.21**	**11%**
Oesophagus	15	31.0	20%	35.1	15%	1.13	25%
	16	50.5	20%	60.1	11%	1.19	23%
	17	59.2	20%	65.1	12%	1.10	23%
	18	64.2	20%	70.9	12%	1.10	23%
	Average	**51.2**	**10%**	**57.8**	**6%**	**1.13**	**12%**

Table 4: Comparison of the measured mean dose of the left lung, right lung and the oesophagus with the corresponding calculated doses for SET 3

SET 3		TLD measurement		PyMCGPU-IR		Calculation/measurement	
Organ	**Slice**	**dose (mGy)**	**U(%) (*k=2*)**	**dose (mGy)**	**U(%) (*k=2*)**	**Ratio**	**U(%) (*k=2*)**
Left Lung	15	8.9	13%	8.7	16%	0.98	21%
	16	86.6	16%	100.3	9%	1.16	19%
	17	106.7	15%	136.5	6%	1.28	16%
	18	89.1	16%	105.8	8%	1.19	18%
	Average	**72.8**	**9%**	**87.8**	**4%**	**1.21**	**10%**
Right Lung	15	53.4	15%	64.4	11%	1.21	18%
	16	11.7	17%	13.2	15%	1.13	23%
	17	-	-	-	-	-	-
	18	16.6	18%	29.8	12%	1.80	22%
	Average	**27.2**	**8%**	**35.9**	**5%**	**1.32**	**10%**
Oesophagus	15	22.5	20%	34.2	16%	1.52	26%
	16	28.2	20%	61.1	12%	2.17	24%
	17	30.2	20%	63.3	13%	2.09	24%
	18	28.4	20%	60.0	13%	2.11	24%
	Average	**27.3**	**10%**	**54.6**	**7%**	**2.00**	**12%**

Differences between calculated and measured doses are within 20% for set 1, set 2 and the left lung in set 3. However, in set 3, the dose calculation for the right lung in slice 18 and the oesophagus in the 4 slices is of the order of a factor of 2. It is believed that this difference is associated to the difficulty in reproducing correctly the position of the phantom in the calculations. Roser et al. [16] performed a study to quantify the uncertainty in organ-equivalent dose in interventional radiology due to marginal displacements of the phantom. They found that longitudinal translations of ±25 mm induced differences ranging from 6% to 135% in the most irradiated organs, whereas the skin dose was almost constant, with a maximum difference of 5%.

In order to analyse the influence of the positioning of the phantom, calculations for set 3 were repeated moving the position of the phantom 7.5 mm in the x-axis (transversal direction) and 15 mm in the z-axis (longitudinal direction). Table 5 presents the results shown in Table 4 for set 3 together with an additional column with the ratio of the new calculations and the measurements in each slice and averaged for each organ.

Table 5: Comparison of the measured mean dose of the left lung, right lung and the oesophagus with the corresponding calculated doses for SET 3, for two positions of the phantom

SET 3		**TLD measurement**	**Ratio:PyMCGPU-IR/TLD**	
			Original (Table 4)	**Displacement**
Organ	**Slice**	**dose (mGy)**	**x=0 mm, z=0 mm**	**x= -7.5 mm, z=15 mm**
Left Lung	15	8.9	0.98	1.06
	16	86.6	1.16	1.48
	17	106.7	1.28	1.41
	18	89.1	1.19	1.36
	Average	**72.8**	**1.21**	**1.41**
Right Lung	15	53.4	1.21	1.54
	16	11.7	1.13	0.94
	17	-	-	-
	18	16.6	1.8	0.98
	Average	**27.2**	**1.32**	**1.34**
Oesophagus	15	22.5	1.52	1.42
	16	28.2	2.17	1.39
	17	30.2	2.09	1.61
	18	28.4	2.11	1.58
	Average	**27.3**	**2.0**	**1.51**

Figure 6 shows the dose distribution and PSD for each set (original positioning of the phantom). During these procedures Gafchromic films were used to evaluate the skin dose distribution. For comparison, the Gafchromic film result for clinical procedure set 2 is shown in Figure 7. A very good agreement between Figure 6 and Figure 7 is observed.

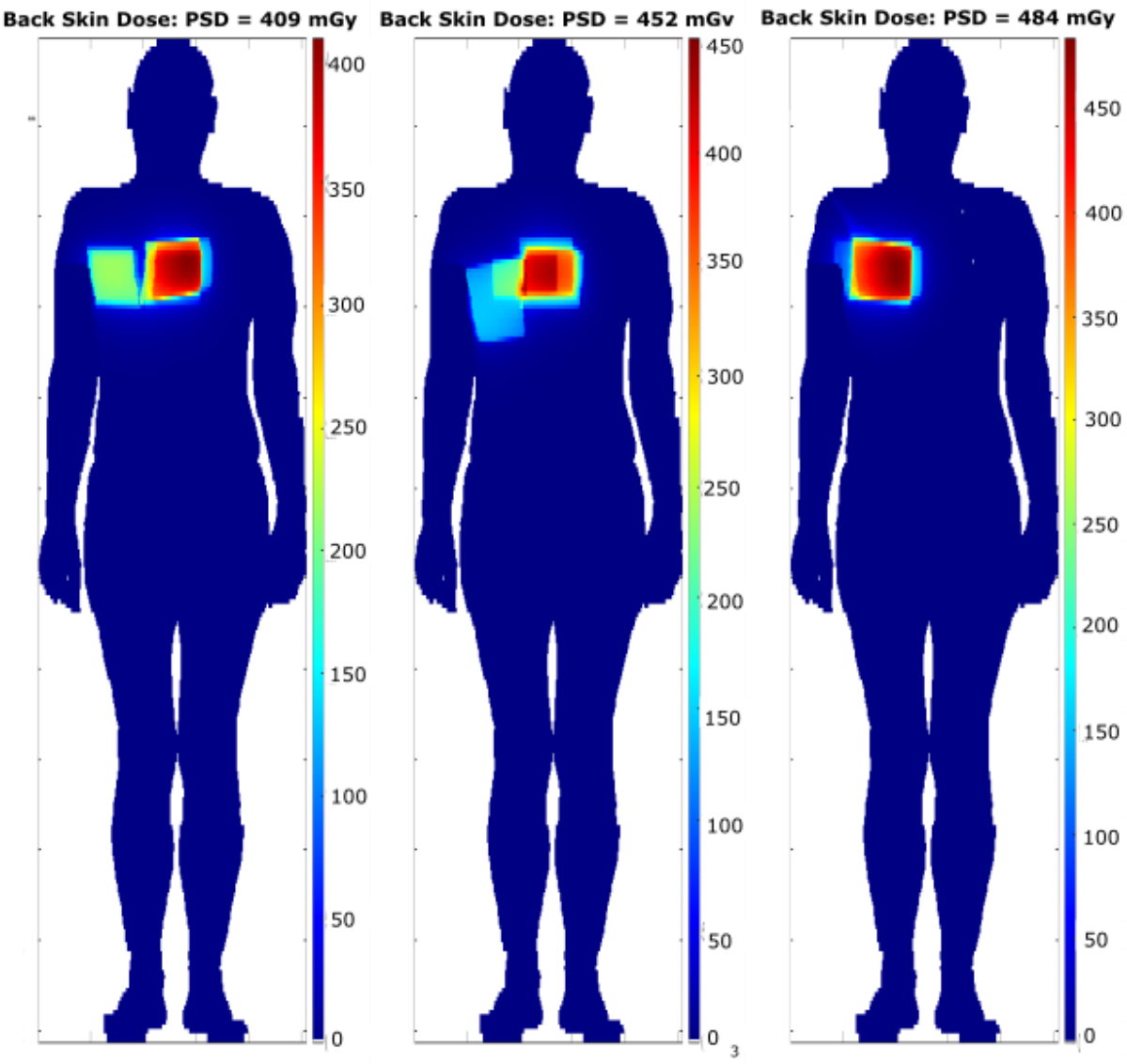

Figure 6: Skin dose distribution for clinical procedures set 1, set 2 and set 3 (from left to right). Voxel size of 0.2137 x 0.2137 x 0.8 cm^3

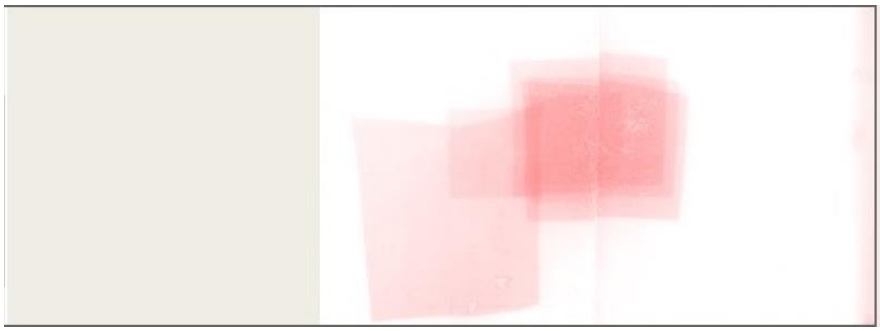

Figure 7: Gafchromic film measurement for clinical procedure SET 2

In order to analyse the influence of the positioning of the phantom in the PSD and mean organ dose, these parameters were calculated for SET 3, for the original position (x=0 mm, z= 0 mm) and with the displacement indicated in Table 5 (x=-7.5 mm, z= 15 mm). Results of the calculations are shown in Table 6 for the PSD, the mean back skin dose and the lung dose. In this case only the organs segmented in the RANDO phantom could be calculated. Thus, in Table 6, the mean lung dose, includes both left and right lung and all the lung voxels, whereas in Tables 2 to 5, the mean left and right lung doses were derived from the average of the doses calculated at the TLD positions.

Table 6: Influence of the positioning of the phantom in the calculated PSD, mean back-skin dose and lung dose for SET 3

SET 3	**PyMCGPU-IR calculated dose (mGy)**		$\frac{dose\ (-7.5\ mm, 15\ mm)}{dose\ (0\ mm, 0\ mm)}$
	x=0 mm, z=0 mm	**x= -7.5 mm, z=15 mm**	
PSD	572	568	0.99
Mean Back-Skin Dose	9.2	8.7	0.95
Mean Lung Dose	35.6	37.5	1.05

Table 6 shows that the impact of the displacement for the PSD, mean skin dose and organ doses is within 5 %. This result is in agreement with the validation results presented in Table 1 and with the conclusions of Roser et al. [16].

4.4 Summary of the validation study

As discussed in 4.3, in the case of the oesophagus, for SET 3, differences are of the order of 100% and 50%, depending on the position of the phantom. This difference is not associated to the performance of PyMCGPU-IR but to the difficulties in centering the phantom and to the fact that there was only 1 TLD to assess the oesophagus dose in each slice. Figure 8 summarizes the results achieved in the different validation tests, without considering the oesophagus.

--

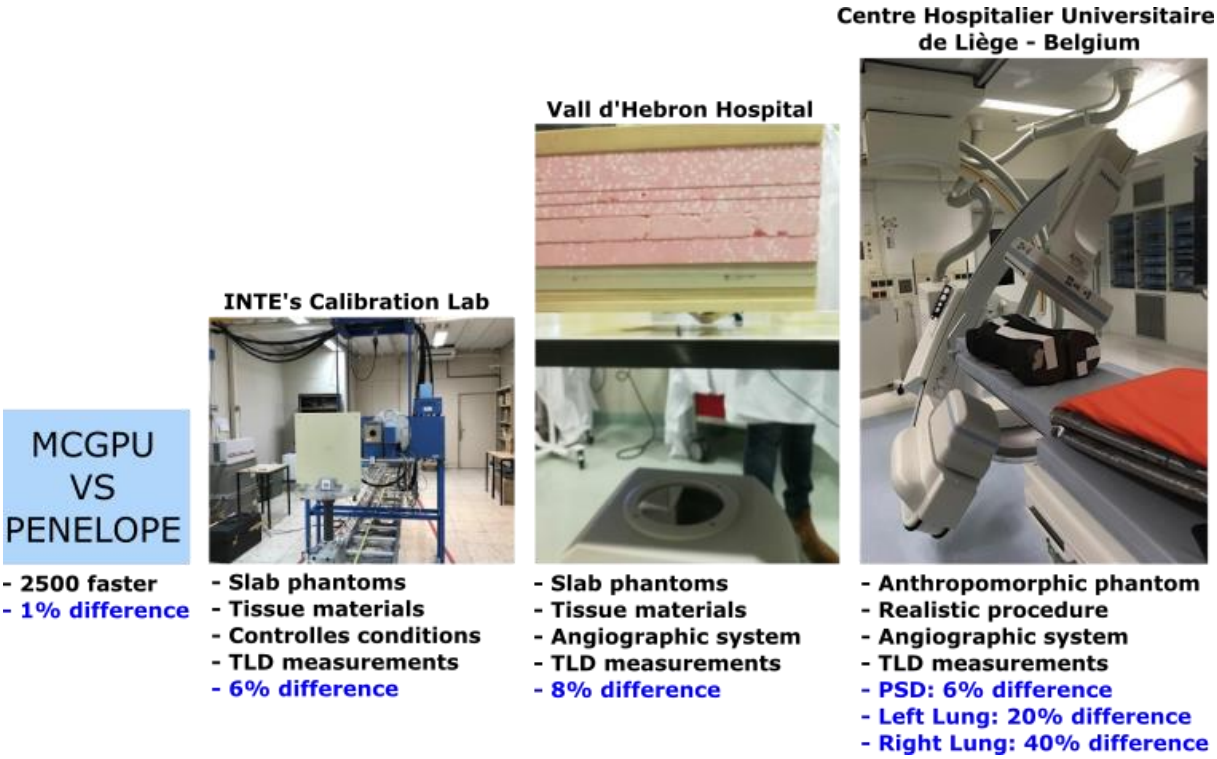

Figure 8: Summary of the different validation experiments

5. PyMCGPU-IR Demo

A Demo of PyMCGPU-IR has been prepared to show how the developed dose patient calculation tool works. In order to simplify the use of PyMCGPU-IR, in case that all the PyMCGPU-IR requirements stated in 3.2 are not available, the demo was designed to be run using a Google Colab spreadsheet. Google Colab is a cloud service, based on Jupyter Notebooks, that allows free use of Google GPUs and, therefore, it can be used to run PyMCGPU-IR. Following few simple instructions, the user will load into the cloud all the source codes needed for PyMCGPU-IR, install it and run an example case of a cardiac clinical procedure (explained below). Once the calculation is finished, the user will obtain on screen the mean and maximum doses for the different tissues and organs of the patient and will be able to download other generated data, such as the different doses per event.

5.1 PyMCGPU-IR Demo requirements.

The user interested in running the PyMCGPU-IR Demo should contact UPC authors: maria.amor.duch@upc.edu and they will be provided with a link to the Google Colab spreadsheet and some simple instructions. The only requirement to run the Demo is to have a Google account.

5.2 Packages for the PyMCGPU-IR Demo.

In order to run PyMCGPU-IR in Goolge Colab the source code of both PyMCGPU-IR and MCGPU-IR have to be loaded into the cloud. Each time the Google Colab is used by a user, the source code has to be loaded. The user will be provided with a set of compressed files containing all the source code as well as user-manual document with all the instructions.

5.3 Description of the radiological case in the Demo

The example case used for this Demo corresponds to a clinical cardiac procedure. It was performed with a Siemens Axiom-Artis Zee angiography system and includes a total of 108 events with different beam energies and shapes as well as different C-arm angulations (set 1 procedure in 4.3).

5.4 PyMCGPU-IR execution and dose retrieval

The Demo is prepared to run in one GPU and the total simulation time (including initialization, calculation and report) will be of about 160 seconds. The programme is set to simulate 10^8 histories per event. For this particular case, the 108 events have been reduced to only 11 events, which has significatively decreased the computational time.

The output that appears on the screen once the simulation is finished is similar to the results shown in Figure 3.

The simulation time in this Demo cannot be compared to the simulations shown in Table 2. In the validation study the number of simulated particles was 10^{10} histories/event. In addition, simulations were done using the UPC cluster, which uses different GPU models than the ones used by Google Colab.

In addition to the screen output, the following files are generated:

- A set of .raw files with the deposited dose per voxel for each event and the total sum of all events.
- A .dat file with the total deposited mean and maximum dose per material.
- A .txt file with all the parameter information of the simulation.

The interested user will be able to access to these files to use the additional data.

6. Conclusions

6.1 Main achievements

It has been proven that PyMCGPU-IR offers high performance and accuracy for dose assessment when compared to standard Monte Carlo codes and TLD measurements. In addition, it should be highlighted that PyMCGPU-IR provides not only the dose values at specific positions, as in the case of the TLDs, but also the dose distribution, the position of maximum dose and the organ doses. In addition, PyMCGPU-IR overcomes the time limitations of CPU-based MC codes.

When compared to other similar software performances [17], PyMCGPU-IR presents some clear advantages as regards its validation against measurements and its independence from the vendor (provided that the required input parameters are available).

Huo et al. [18] compared VirtualDoseIR (Virtual Phantoms Inc., Albany, New York, USA) organ dose results with measurement data previously published and found differences of 40%. Regarding skin dose estimations, differences between 15 % and 76% have been reported in previous studies [19, 20, 21].

6.2 Further work

Real time dose calculation

At present, due to the lack of access to the radiation source information in real time, PyMCGPU-IR has been developed to perform calculations once the procedure is finished. However, should this information be available, the programme could be easily adapted. First of all, one should load the patient geometry and materials before starting irradiating the patient. Once the program has started, each irradiation event needs to be notified, converted and notified to MCGPU-IR. The access to RDSR is not needed anymore. Finally, as regards, the present clustering algorithm, a *cache*[5] match could be implemented by using similar rules to compare events [3].

Skin Dose Viewer

For the sake of a better user interface and an easier patient dose interpretation, a tool that automatically reads the retrieved data from PyMCGPU-IR and generates a picture of the skin dose distribution is under progress and will be implemented in a new version of PyMCGPU-IR (2021).

Patient position in the table

The reliability of the dose calculation is dependent on patient's position on the table. Unfortunately, the position of the patient is not standardized and it is often difficult to record. The same problem is found in any similar software tool. One possible approach to overcome this problem is to use one of the images to improve the matching between the simulated and the experimental geometry.

[5] Cache: an auxiliary memory from which high-speed retrieval is possible.

7. References

1. European Commission 2013. Council Directive (Euratom 2013/59) laying down basic safety standards for protection against the dangers arising from exposure to ionising radiation. Off. J. Eur. Commun. 2014.
2. Badal A. and Badano A., Accelerating Monte Carlo simulations of photon transport in a voxelized geometry using a massively parallel Graphics Processing Unit, Medical Physics 36, pp. 4878–4880 (2009).
3. von Barnekow A., Fernández Bosman D., Ginjaume M., Duch M.A. Automatic acquisition of X-ray source conditions from console module in interventional cardiology. MEDIRAD WP2 Milestone 41, July 2020.
4. Fernández Bosman D., García Balcaza V., Delgado C., Principi S., Duch MA., Ginjaume M. Validation of the MC-GPU Monte Carlo code against the PENELOPE/ penEasy code system and benchmarking against experimental conditions for typical radiation qualities and setups in interventional radiology and cardiology. Physica Medica 82 (2021) 64–71.
5. Salvat F, Fernandez-Varea JM, and Sempau J. PENELOPE 2006: A code system for monte carlo simulation of electron and photon transport. Workshop Proceedings Barcelona, Spain, 4-7 July 2006, OECD 2006 NEA No.6222, 2006.
6. PENELOPE-2014: A Code System for Monte Carlo Simulation of Electron and Photon Transport; NEA/NSC/DOC(2015)3; Workshop Barcelona, Spain 29 June-3 July 2015
7. NEMA PS3 / ISO 12052, Digital Imaging and Communications in Medicine (DICOM) Standard, National Electrical Manufacturers Association, Rosslyn, VA, USA (available free at http://www.dicomstandard.org/).
8. Schlattl, H., et al., Organ dose conversion coefficients for voxel models of the reference male and female from idealized photon exposures, Physics in Medicine and Biology 52 (2007) 2123-2145.
9. Zankl, M., et al., Voxel-based models representing the male and female ICRP reference adult – the skeleton, Radiation Protection Dosimetry 127 1-4 (2007) 174-186.
10. ICRP, 2009. Adult Reference Computational Phantoms. ICRP Publication 110. Ann. ICRP 39 (2).
11. Joint Committee for Guides in Metrology. Evaluation of measurement data — Guide to the expression of uncertainty in measurement. JCGM 100:2008 GUM 1995 with minor corrections. Available in: https://www.bipm.org/utils/common/documents/jcgm/JCGM_100_2008_E.pdf.
12. Sempau J, Badal A, Brualla L. A PENELOPE-based system for the automated Monte Carlo simulation of clinacs and voxelized geometries-application to far-from-axis fields. Med Phys 2011;38:5887–95. doi:10.1118/1.3643029.
13. IT'IS Foundation. Virtual population, https://itis.swiss/virtual-population/virtual-population/overview/
14. International Electrotechnical Commission, Medical diagnostic X-ray equipment - radiation conditions for use in the determination of characteristics, IEC 61267, IEC, Geneva (2005).
15. White DR, Booz J, Griffith RV, Spokas JJ, Wilson IJ, Report 44. Tissue substitutes in radiation dosimetry and measurement. Journal of the International Commission on Radiation Units and Measurements. 1989, 23, 1, https://doi.org/10.1093/jicru/os23.1.Report44
16. Roser P., Birkhold A., Zhong X., Ochs P. et a. Pitfalls in interventional X-ray organ dose assessment—combined experimental and computational phantom study: application to prostatic artery embolization. International Journal of Computer Assisted Radiology and Surgery, 14, (2019) 1859–1869. https://link.springer.com/article/10.1007%2Fs11548-019-02037-6
17. F. Malchair, J. Dabin, M. Deleu, M. Sans Merce, O. Ciraj Bjelac, A. Gallagher, C. Maccia. Review of skin dose calculation software in interventional cardiology. Physica Medica 80 (2020) 75–83.
18. Huo W, Pi Y, Feng M, et al. VirtualDose-IR: a cloud-based software for reporting organ doses in

interventional radiology. *Phys Med Biol*. 2019;64(9):095012. https://doi.org/10.1088/1361-6560/ab0bd5.

19. Järvinen J, Sierpowska J, Siiskonen T, Husso M, Järvinen H, Kiviniemi T, et al. Contemporary radiation doses in interventional cardiology: A nationwide study of patient skin doses in finland. Radiat Prot Dosimetry 2020;188:181–90. https://doi.org/10.1093/rpd/ncz273.
20. Greffier J, Van Ngoc Ty C, Bonniaud G, Moliner G, Ledermann B, Schmutz L, et al. Assessment of peak skin dose in interventional cardiology: A comparison between Gafchromic film and dosimetric software em.dose. Phys Medica 2017;38:16–22. https://doi.org/10.1016/j.ejmp.2017.05.044.
21. Bordier C, Klausz R, Desponds L. Accuracy of a dose map method assessed in clinical and anthropomorphic phantom situations using gafchromic films. Radiat Prot Dosimetry 2015;165:244–9. https://doi.org/10.1093/rpd/ncv034.

8. Acknowledgments

The authors gratefully acknowledge the interesting and helpful assessment and discussions with Andreu Badal, for MC-GPU improvements and with Françoise Malchair, for the realistic measurement. They also appreciate the valuable contributions of the UPC master students Anna Torras and Alvaro Merino, as well as the collaboration of staff at the UPC Laboratory and HUVH and Liege hospitals where experimental work was carried out.